STAR Protocols

CellPress
OPEN ACCESS

Protocol

A pipeline for STED super-resolution imaging and Imaris analysis of nanoscale synapse organization in mouse cortical brain slices

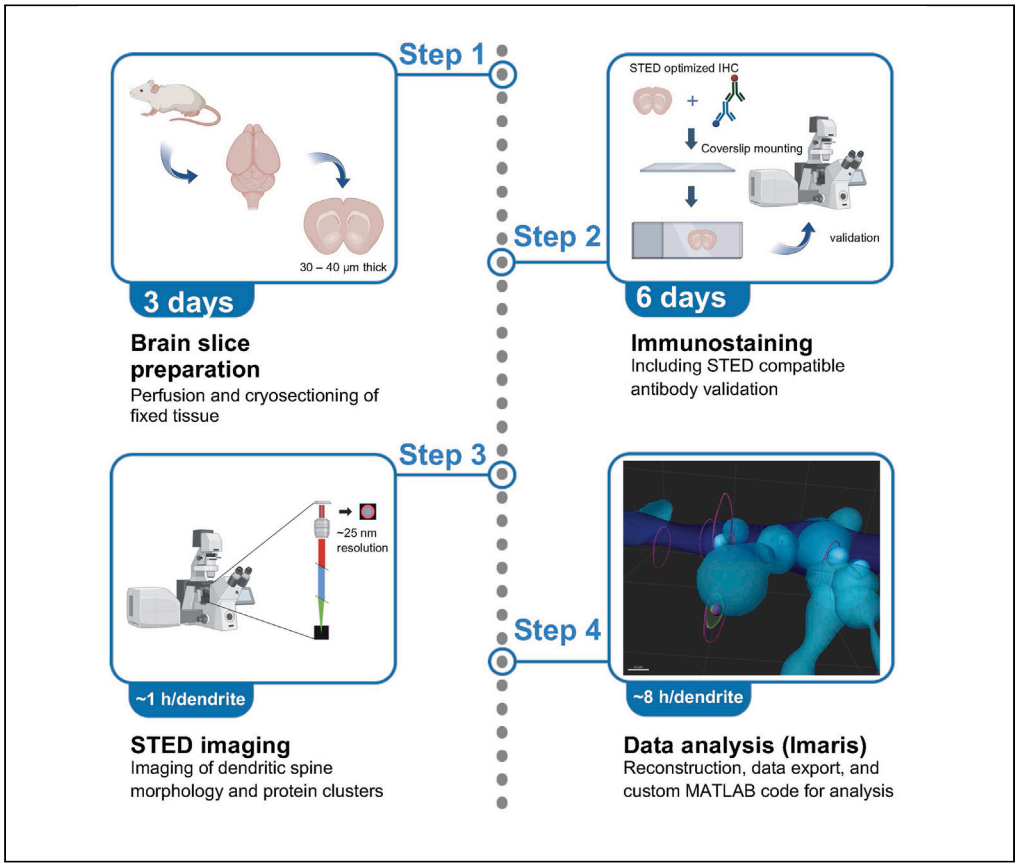

Advances in super-resolution imaging enable us to delve into its intricate structural and functional complexities with unprecedented detail. Here, we present a pipeline to visualize and analyze the nanoscale organization of cortical layer 1 apical dendritic spines in the mouse prefrontal cortex. We describe steps for brain slice preparation, immunostaining, stimulated emission depletion super-resolution microscopy, and data analysis using the Imaris software package. This protocol allows the study of physiologically relevant brain circuits implicated in neuropsychiatric disorders.

Publisher's note: Undertaking any experimental protocol requires adherence to local institutional guidelines for laboratory safety and ethics.

Ezra Kruzich, Rhushikesh A. Phadke, Alison Brack, Dimitri Stroumbakis, Oriannys Infante, Alberto Cruz-Martín

ezrak@bu.edu (E.K.)
martini.cruz@gmail.com (A.C.-M.)

Highlights

Outlines a detailed tissue preparation protocol for STED super-resolution microscopy

Includes a comprehensive guide for optimization of image acquisition parameters

Utilizes STED super-resolution imaging and a custom Imaris/MATLAB analysis pipeline

Determines the nanoscale protein organization within mouse prefrontal cortex slices

Kruzich et al., STAR Protocols 4, 102707
December 15, 2023
https://doi.org/10.1016/j.xpro.2023.102707

STAR Protocols

CellPress
OPEN ACCESS

Protocol

A pipeline for STED super-resolution imaging and Imaris analysis of nanoscale synapse organization in mouse cortical brain slices

Ezra Kruzich,[1,5,*] Rhushikesh A. Phadke,[2] Alison Brack,[2] Dimitri Stroumbakis,[1] Oriannys Infante,[3,4] and Alberto Cruz-Martín[1,2,6,*]

[1]Neurobiology Section in the Department of Biology, Boston University, Boston, MA 02215, USA

[2]Molecular Biology, Cell Biology, and Biochemistry Section in the Department of Biology, Boston University, Boston, MA 02215, USA

[3]Montclair State University, Montclair, NJ 07043, USA

[4]Summer Undergraduate Research Fellowship Program, Boston University, Boston, MA 02215, USA

[5]Technical contact: ezrak@bu.edu

[6]Lead contact

*Correspondence: ezrak@bu.edu (E.K.), martini.cruz@gmail.com (A.C.-M.)
https://doi.org/10.1016/j.xpro.2023.102707

SUMMARY

Advances in super-resolution imaging enable us to delve into its intricate structural and functional complexities with unprecedented detail. Here, we present a pipeline to visualize and analyze the nanoscale organization of cortical layer 1 apical dendritic spines in the mouse prefrontal cortex. We describe steps for brain slice preparation, immunostaining, stimulated emission depletion super-resolution microscopy, and data analysis using the Imaris software package. This protocol allows the study of physiologically relevant brain circuits implicated in neuropsychiatric disorders.

BEFORE YOU BEGIN

While neuroscientists have taken various approaches to investigate the nanoscale protein organization of the synapse using Stimulated Emission Depletion (STED) nanoscopy[1–3] and the interactive microscopy image analysis software Imaris (Oxford Instruments, Abingdon, United Kingdom), this protocol uses specific fundamental principles of labeling, data collection, and analysis to characterize the morphological features of brain cell types and determine the localization of proteins within subcellular compartments or colocalization of two proteins in physiologically relevant circuits using fixed brain slices.

We designed this protocol to investigate three primary questions.

1. What is the density and morphology of dendritic spines in apical tufts of cortical layer (L) 2/3 pyramidal cells in the mouse prefrontal cortex (PFC)?
2. What is the proportion of α-amino-3-hydroxy-5-methyl-4-isoxazolepropionic acid (AMPA) GluR1 subunit clusters localized to lysosome-associated membrane protein 1 (LAMP1)-positive lysosomes within specific dendritic compartments?
3. What is the nanoscale organization of specific synaptic and lysosomal proteins within dendritic sub-compartments?

In pursuit of these questions, we utilize the following specific approaches.

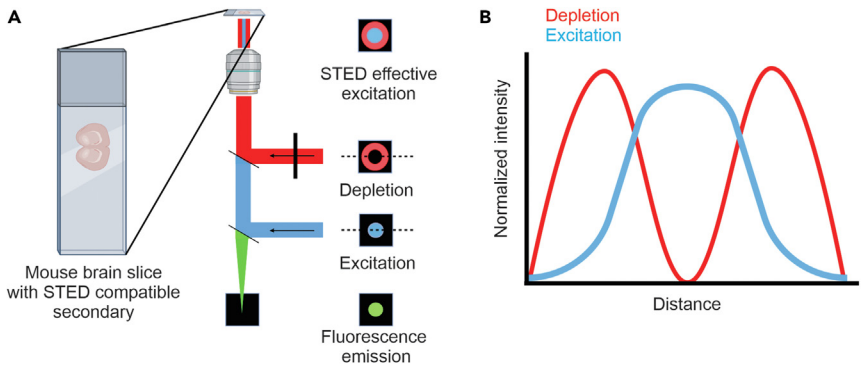

Figure 1. Experimental setup and STED microscopy basics

(A) Basic experimental setup and principles of STED microscopy. Mouse brain slices are stained with STED compatible secondaries and subjected to both excitation and depletion beams, resulting in fluorescence emission of reduced size.

(B) Pseudo-graph for visualization of normalized intensity as a function of distance along the dotted lines across the depletion (red) and excitation (blue) beams shown in (A)..

4. The use of fixed brain slices: Fixed brain slices maintain the natural 3D structure and architecture of the brain, allowing researchers to study the spatial relationships between different cell types, regions, and structures.[4] This is particularly valuable for understanding connectivity and circuitry within the brain. Fixed brain tissue mirrors *in vivo* conditions more accurately than dissociated neuronal cultures. This is important for investigating processes that are influenced by the overall environment of the brain, such as developmental changes, neurodegeneration, and immune responses. It should be noted that fixation can affect the 3D structure of cells and tissues in ways that could alter the immunostaining results. For more information regarding potential solutions, please see 'tissue fixation' in the limitations section.
5. The use of genetic labeling with fluorescent proteins to image neuronal morphology: We optimized this protocol using *in utero* electroporation (IUE) for sparse genetic labeling of L2/3 pyramidal in the medial (m) PFC with EB.[4,5] However, this protocol can be adapted to label neurons and other brain cell types with far-red to near-infrared fluorescent proteins, such as TagRFP657, mNeptune2, mGarnet and mGarnet2.[6] Additionally, this protocol can be adapted with the use of bright fluorescent dyes, including Alexa Fluor 488,[7] Alexa Fluor 594,[8] and Oregon Green 488 dye.[9] Bolus loading with Alexa Fluor 488 can label pyramidal cells and dendritic processes in brain slices[10,11] without using fluorescent proteins.
6. The use of synaptic and lysosomal markers: In this protocol, we performed immunohistochemistry (IHC) for the lysosomal marker LAMP1[12,13] and the AMPA glutamate receptor subunit GluR1.[14,16]
7. The use of super-resolution imaging: In this protocol, we utilized techniques that enable resolution of structures below the diffraction limit of light.[17] This diffraction limit refers to the smallest feature size that can be resolved by an optical imaging system due to restraints imposed by the physics of light. This limit is approximately 250 nm laterally for a light microscope, with an axial resolution limit of around approximately 500–700 nm depending on the wavelength.[18] The typical STED experimental setup uses a confocal laser scanning microscope equipped with an additional depletion beam with a "donut" shaped intensity profile (Figure 1A).[17,19,20]

The STED donut is aligned with the diffraction limited excitation spot, depleting or turning off the excited fluorophores at the periphery of the excitation spot, allowing only those fluorophores in the hole of the STED donut to fluoresce spontaneously (Figure 1A).[17,19,20] This reduces the area of detectable fluorescence and drastically improves the lateral resolution (Figure 1B).[17,19,20] The STED resolution can be described with the following equation:

$$d \approx \lambda \Big/ \left(2NA\sqrt{1+I/Is}\right).$$

where *NA* refers to the numerical aperture, *I* represents the maximum intensity of the STED beam, and *Is* refers to the intensity when the depletion beam deactivates a fraction of the fluorescent molecules.[21] For more details regarding these relationships, please see Wildanger et al.[21] This protocol is optimized for the Abberior Facility Line STED experimental setup (Abberior GmbH, Göttingen, Germany) but also describes a general approach to multiple STED imaging contexts. A more in-depth discussion of STED super-resolution microscopy can be accessed elsewhere.[1,6,17,19,22]

Institutional permissions

Investigators must obtain institutional permission to perform animal studies and collect tissues under an approved Institutional Animal Care and Use Committee (IACUC) or Institutional Review Board protocol. All experimental protocols were conducted according to the National Institutes of Health (NIH) guidelines for animal research and were approved by the Boston University Institutional Animal Care and Use Committee (IACUC; protocol #201853).

Perfusion

Timing: ~30 min for preparation and first mouse, <=20 min/additional mouse

This step describes the basic process of perfusing the mouse, fixing the brain, and preparing the tissue for slicing. For a more detailed protocol, please see Wu et al.[23]

8. Administer an overdose of sodium pentobarbital to the animal intraperitoneally.
9. Transcardially perfuse with phosphate buffered saline (PBS) then 4% paraformaldehyde (PFA) in PBS.
10. Extract brain and postfix in 4% PFA for 24 h.
11. Transfer to 30% (w/v) sucrose solution and store at 4 °C for at least 24 h.

Note: We typically perfuse mice at a rate of 5 mL/min (Step 2).

Sectioning of tissue

Timing: ~1 h for preparation and first mouse, <=30 min/additional mouse

This step describes the process of sectioning the tissue for STED imaging experiments. The user should be aware that the mismatch in refractive index between the optics of the STED microscope and the tissue leads to optical aberration, which induces distortions on the laser wavefront that can severely degrade the quality of the STED point spread function (PSF).[1,24]

⚠ CRITICAL: Thus, a key principle for the ensured success of a STED imaging experiment is to decrease the thickness of the tissue. Our protocol restricts slice thickness to approximately 30–40 μm, allowing us to obtain 30 μm long horizontally aligned dendritic shafts, which reduces spine density variability between dendrites.

Note: In this protocol, we are extracting and processing brain tissue to isolate the mouse mPFC.

12. Adequately crush dry ice into small pieces and apply to stage until stage is fully frozen (approximately 5–10 min for freezing platform).
13. Use a small amount of OCT compound to mount the caudal part of the brain to the stage (with cerebellum removed), with olfactory bulbs pointing upwards and the cortex facing the blade.
14. Apply crushed dry ice on and around the brain for approximately 5 min or until brain is fully frozen.
15. Remove dry ice from the brain and section at a thickness of approximately 30–40 μm.

16. Using a point brush to gently remove slices from the blade and add them to 24-well plate with 1× PBS.
17. Add one slice per well in succession (each well should have 1 mL of 1x PBS).
18. Once each well of the plate has three slices, use a new a new plate.
19. Store slices at 4 °C.

Note: Although cutting thinner tissue will improve the STED optics, in our context it reduces the probability of imaging horizontally aligned dendritic shafts that are more than 30 μm, which is critical to reduce spine density variability between dendrites.

Note: If the slices are not used within 8 h, add sodium azide (0.02%–0.1%) to 1 x PBS) to the PBS solution for long-term storage (Step 8).

⚠ CRITICAL: To ensure optimal slice integrity, it is important to avoid temperature fluctuations during slicing, which can be achieved by keeping a supply of quality dry ice on hand, applying small amounts to the stage and around the brain throughout the procedure.

Antibody selection

Timing: 1–3 h, depending on antibody availability

Primary antibodies should be selected based on their published efficacy for IHC in mouse brain slices. Secondary antibody selection is most important for STED imaging: the technique's depletion technology acts on the secondary, so careful selection is vital for quality images. We optimized this protocol for secondary antibodies selected according to compatibility with Abberior Facility Line STED microscopy applications.

Note: The most important factor in successful antibody selection is to perform a literature search to confirm published results. This is essential because unspecific or bad antibody batches are often sold under different names and catalog numbers, giving the impression that they are different antibodies.

⚠ CRITICAL: To perform successful STED super-resolution imaging of two or more signals requires careful selection of fluorophores with well-separated emission spectra, ensuring compatibility with STED conditions and photostability.[25–27] Thorough validation, control experiments, and expert knowledge of STED microscopy techniques and data analysis contribute to achieving accurate, high-resolution imaging outcomes.

Antibody validation

Timing: 6 days

20. To determine the optimal primary antibody concentration, perform a dilution series with the manufacturer's recommended concentration, a more diluted option, and a more concentrated option, holding the secondary antibody concentration constant according to the manufacturer's recommendation.[28]
    a. Collect confocal images of each dilution.
    b. Assess staining efficacy with FIJI/ImageJ (NIH, Bethesda, MD) or another image processing software.

Note: We recommend optimizing initial imaging parameters using the mid-range dilution. For more details regarding imaging parameters, please see the "optimizing confocal imaging parameters guide" section below.

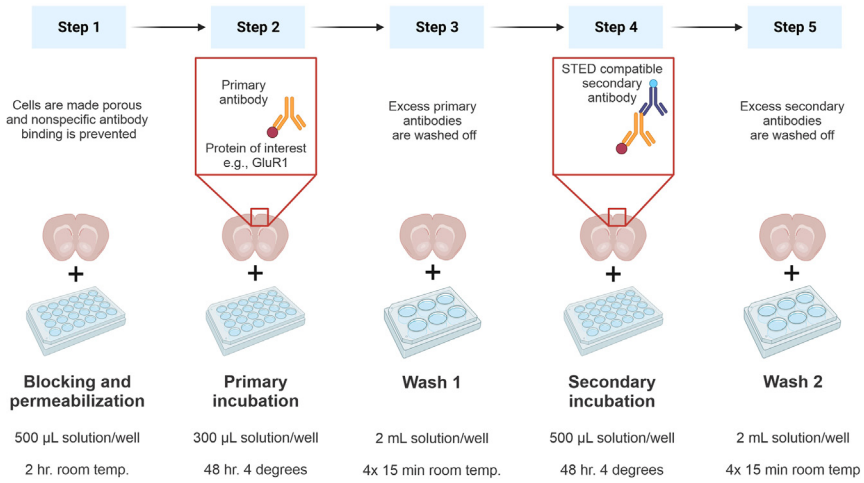

Figure 2. Schematic of IHC steps and important details

Brain slices, explanations of solution functions and proper plate choice (24 or 6 well) at each step are represented. We advise researchers to keep note of changes in solution volumes, shaking temperatures throughout the protocol, and the use of a 6-well plate for steps 3 and 5 as opposed to the 24-well plate used in steps 1, 2, and 4.

21. To determine the optimal secondary antibody concentration, perform another dilution series, holding the selected primary concentration from step 1 constant, then using the manufacturer's recommended concentration, a more dilute option, and a more concentrated option.
    a. Acquire confocal images of each dilution and assess staining efficacy with FIJI/ImageJ (please see step 1.a, b, for our recommended approach).
        i. Repeat steps 1 and 2 as needed according to each analyzed result.
22. To assess negative controls, prepare a condition with only primary antibody and no secondary as well as a condition with only secondary and no primary, otherwise performing all other steps of the IHC protocol as described below.
    a. Compare these results with each dilution using the strategy described above.
23. Compare antibody results with published use of the antibody in rodent brain slices to ensure antibody specificity.

Note: Antibody specificity should be confirmed in brain tissue by using KO transgenic mouse lines and by performing staining experiments in HEK293 cells with negative and positive controls.

Note: Keeping the effects of the depletion in mind,[29] we recommend using antibody concentrations that result in strong signal-to-noise ratio (SNR), finding that this works best for STED imaging.

Immunohistochemistry

Timing: 2–3 h, every other day for 6 days total

Please see Figure 2 for a schematic of the IHC steps.

24. To prepare for immunostaining, block and permeabilize slices in a blocking buffer (10% donkey serum + 1% Triton X100) in a 24-well plate; 500 µL per well.
25. Incubate 180 min at room temperature on a shaker.
26. Incubate slices with primary antibody(ies) in a 24-well plate: 300 µL of 1x PBS + 0.025% Triton X100 with 10% donkey serum and primary antibody(ies).
27. Wrap plate with parafilm or plastic wrap to avoid evaporation.

28. Incubate for 48 h in 4 °C cold room on a shaker.
29. Remove primary antibody solution.
30. Wash slices for 14 min 4 × with 2 mL 1x PBS + 0.025% Triton X-100 in a 6-well plate.
31. Incubate with secondary antibody(ies) in a 24-well plate: 500 μL of 1x PBS and secondary antibody(ies).
32. Wrap plate with parafilm or plastic wrap to avoid evaporation.
33. Cover plate with an opaque material (aluminum foil or thick cardboard box) to avoid photobleaching of fluorescent probes.
34. Incubate for 48 h in 4 °C cold room on a shaker.
35. Remove secondary antibody solution.
36. Wash slices for 15 min 4 × with 2 mL 1x PBS in a 6-well plate.

Note: If the background is high when imaging, additional washes may improve the signal (Step 13).

Mounting

Timing: ~10–15 min/slide

37. Mount slices with a DAPI-less mounting media that matches the refractive index of the objective as closely as possible, in our case Diamond Fluoromount (see key resources table).

CRITICAL: Mounting media including DAPI, or other dyes can interfere with the coordination between emission and depletion lasers (e.g., DAPI might be excited by the STED laser, leading to increased background), so STED microscopy must be performed with a DAPI-less mounting media.

Note: It is important to note that homogeneity of an imaging environment's refraction index helps ensure high penetration depth and minimizes aberrations. This can be helped by using mounting media with a refractive index that matches the immersion medium of the objective.

38. Using a paintbrush, gently slide the brush underneath the tissue and lift the brain slice from the plate.
39. To mount the brain slice, press the right side of the brush to the side of a 1.5 mm coverslip and slowly roll the brush clockwise.

CRITICAL: The next step in limiting sample-to-objective distance is to mount the brain slices onto the coverslip, not the slide, so the tissue is closer to the objective than the mounting media. The DAPI-less mounting media is preferable to the alternative but can still interfere with the localization of the STED donut, further necessitating the coverslip mounting.

40. Use the 1x PBS saturated brush to gently adjust the tissue so it is flat on the coverslip.
41. Let slices dry approximately 30 min (until they appear crystalline and mostly translucent).
42. Apply approximately 100 μL of mounting media to the slide, forming a perpendicular line of media adjacent to the label and a parallel line down the slide forming a "T" shape.
43. Place one side of the coverslip onto the top of the T, then slowly lower the other side.
44. Cover the mounted slides to avoid photobleaching and then dry overnight before they are used.

Note: To increase SNR during STED imaging, it is essential to decrease non-specific background fluorescence. Several actions that can be taken to reduce autofluorescence, namely: performing negative staining controls (see 'antibody validation' section), prioritizing fluorophores that emit a wavelength farther from the emission of autofluorescent endogenous

molecules and pigments of the tissue (such as far-red selections),[30] and using background reducers such as TrueBlack, Sudan black B, or Eriochrome black T.[31]

Note: Optical aberrations can be further reduced by combining STED with tissue-clearing approaches, typically performed when mounting the slice.[24]

Optimizing confocal imaging parameters guide

Timing: ~10–15 min

When utilizing fluorescence microscopy techniques, achieving a good SNR while avoiding fluorophore saturation is essential for obtaining high-quality images. We recommend consulting this guide of empirical methods and tips prior to and throughout imaging experiments to ensure a good SNR without fluorophore saturation.

45. Monitor pixel intensity.
    a. Capture an image of the sample and inspect the histogram of pixel intensities in the confocal acquisition software.

Note: A good SNR image should have a well-distributed histogram without a significant portion of pixels reaching the maximum intensity value (i.e., saturation).

46. Optimize laser power.
    a. Start with lower laser power and gradually increase it while monitoring the image quality.
    b. Look for the point at which increasing laser power results in no further increase in signal intensity (a plateau). This is the optimal power level to prevent saturation while maximizing SNR.
47. Adjust pinhole size.

Note: A smaller pinhole allows the capture of light only from a very thin optical section, reducing background noise although potentially lowering signal intensity. A larger pinhole captures more light, increasing signal intensity with the opposite effect on background noise.

Note: We recommend experimenting with different pinhole sizes to find those that best accommodate one's imaging needs.

48. Adjust gain and offset adjustment.

Note: The gain amplifies the signal, while the offset sets the baseline for the image.

49. Perform an average of multiple frames during image acquisition to reduce noise while increasing signal intensity.

Note: This may help prevent saturation due to the averaging out of noise as the signal accumulates.

50. Choose a region of interest (ROI).

Note: Some imaging applications are best suited for focus on a specific region of interest rather than imaging the entire field of view. Reducing the imaging area can increase the SNR for specific structures of interest.

51. Monitor signal intensity.

Note: It is important to monitor the signal intensity over time during image acquisition. If the intensity begins to plateau or decrease after a certain point, it may indicate fluorophore saturation. Adjust settings accordingly.

52. Optimize secondary antibody concentration.

Note: Optimizing lower-concentration secondary antibody solutions can help reduce the chances of saturation due to the dilution of fluorophores. However, this may require longer exposure times to achieve a sufficient SNR.

53. Use appropriate controls.

Note: Always include negative controls (e.g., samples without fluorophores) and positive controls (e.g., samples with known fluorophore concentrations) to validate your imaging conditions and assess SNR.

54. Perform pilot experiments.

Note: As mentioned in multiple contexts throughout this protocol, we highly recommend conducting pilot experiments with various settings and conditions to determine the most optimal parameters for one's imaging needs.

KEY RESOURCES TABLE

REAGENT or RESOURCE	SOURCE	IDENTIFIER
Antibodies		
Anti-GFAP (mouse) (dilution: 1:250)	Novus Biologicals	NBP22239
Anti-LAMP1 (rabbit) (dilution: 1:500)	Abcam	Ab24170
Anti-PSD95 (mouse) (dilution: 1:500)	Rockland	600-301-215M
Anti-mouse Abberior STAR Orange (dilution: 1:300)	Fisher Scientific	NC1993863
Anti-rabbit Abberior STAR Red (dilution: 1:1000)	Fisher Scientific	NC1993780
Chemicals, peptides, and recombinant proteins		
Phosphate-buffered saline 10×	Boston BioProducts	BM-220, 7001104
Paraformaldehyde (PFA)	Sigma-Aldrich	158127-500 g
Sucrose	Bio Basic	SB0925
Donkey serum	Sigma-Aldrich	S30-100 mL
Triton X100	Sigma-Aldrich	9036-19-5
ProLong Diamond antifade mountant	Thermo Fisher Scientific	P36961
Sodium pentobarbital	Virtech Pharmaceuticals	07-801075
Scigen Tissue-Plus O.C.T. compound	Fisher Healthcare	27-730-571
Sodium azide	Sigma-Aldrich	S2002-100 g
Critical commercial assays		
ZymoPURE II	Zymo Research	D4208
Experimental models: Organisms/strains		
CD-1 IGS mouse (wild type, postnatal day (P) 125, male and female mice)	Charles River	Strain code 022
Recombinant DNA		
EGFP under the CAG promoter	Addgene	Plasmid #11150
Software and algorithms		
Imspector	Abberior Instruments GmbH	Imspector Image Acquisition & Analysis Software v16.3 https://imspector.abberior-instruments.com/
ImageJ software (Fiji)	Schneider et al., 2012	https://imagej.nih.gov/ij/

(*Continued on next page*)

Continued

REAGENT or RESOURCE	SOURCE	IDENTIFIER
MATLAB	MathWorks	RRID: SCR_001622
Imaris 9.7 or higher	Oxford Instruments	RRID: SCR_007370
Spots close to filament border Imaris Xtension	Imaris Open	https://imaris.oxinst.com/open/
Colocalize spots Imaris Xtension	Imaris Open	https://imaris.oxinst.com/open/
GitHub README file	GitHub	https://github.com/CruzMartinLab/IMARIS_compiler
Other		
Sliding microtome	Leica	SM2000
Peristaltic pump	Masterflex C/L dual-channel tubing pump	Cole Parmer
Inverted laser scanning confocal microscope (Nikon Ti2 with perfect focus, P736 Piezo Z-stage with an Abberior Facility Line STED system controlled with the Abberior Imspector software platform)	Nikon Instruments, Abberior GmbH, and Physik Instrumente	N/A
Plan apochromat 60 × 1.4 N.A. oil immersion objective	Nikon Instruments	N/A
1 mm coverslips	Corning	2975-225

MATERIALS AND EQUIPMENT

Materials and equipment	Source	Identifier
Sliding microtome	Leica	SM2000
Peristaltic pump	Masterflex C/L Dual-Channel Tubing Pump	Cole Parmer
Inverted laser scanning confocal microscope (Nikon Ti2 with perfect focus, P736 Piezo Z-stage with an Abberior Facility Line STED system controlled with the Abberior Imspector software platform	Nikon Instruments, Abberior GmbH, and Physik Instrumente	N/A
Plan apochromat 60 × 1.4 N.A. oil immersion objective	Nikon Instruments	N/A

STEP-BY-STEP METHOD DETAILS

Imaging

Timing: ~30 min to 1 h/image

Our experimental design utilizes genetic labeling of L2/3 pyramidal cells with the fluorescent protein EGFP to study neuronal morphology (**Question 1**). In our protocol, confocal imaging of the EGFP is necessary to determine the localization and nanoscale organization of various proteins in dendritic structures.

Note: The user should know that in this case EGFP's natural fluorescence response is not conducive to super-resolution imaging due to its relatively broad emission spectrum and susceptibility to photobleaching.[32] Once ROIs and Z-stacks are selected according to the dendrite of choice, STED parameters may be optimized for the resulting puncta clusters in each channel of interest (in our case GABA$_B$R1 and LAMP1, please see the "optimizing confocal imaging parameters guide" section above).

Note: Excitation power should be initially set so that averaging of the signal results in adequate visualization of dendritic spines for accurate morphological reconstructions. This will result in an image most suitable for Imaris digital reconstruction. Excitation and STED power should be set so that averaging of the signal results in bright low background images without danger of bleaching. Before beginning an experiment, the user should determine

empirically optimized imaging parameters of each dye or fluorescent protein. Please see "optimizing confocal imaging parameters guide" for more information.

⚠ CRITICAL: To reduce optical aberrations, the user should image superficial dendrites, preferably within the first 10–15 μm of the tissue. Additionally, the user should image horizontally aligned dendrites, where most of the dendritic shaft is contained within a few optical sections.

Note: Imaging the morphology of dendritic structures with nanoresolution can be accomplished by using secondary antibodies that are conjugated with STED compatible fluorophores (described later). However, in our protocol, because of the limited availability of channels, this is not compatible with protein cluster colocalization experiments.

Note: For imaging, we use an inverted laser scanning confocal microscope with 60 × 1.4 NA oil immersion objective (Nikon, Tokyo) outfitted with an Abberior Facility Line STED system controlled with the Abberior Imspector software platform.

1. To begin imaging, select 488 nm (for EGFP IUE cell fill), 561 nm (Abberior STAR Orange for GFAP), and 640 nm (Abberior STAR Red for LAMP1) pulsed excitation lasers lines.
2. Select 775 nm STED depletion laser (Abberior STAR Orange, Abberior STAR Red) line.
3. Select ROIs localized to L1 apical dendritic tufts from L2/3 pyramidal cells in the mPFC. To find the best ROI:

Note: Maintain a strict selection criterion when imaging the morphology and density of dendritic spines in the cerebral cortex. In our experience, we have observed significant variability in spine density between apical and basal dendrites and dendritic spine segments of different dendritic branch orders[4,10,33] and in how genetic manipulations affect specific dendritic types.[4] It should be noted that L1 apical tufts are mostly within the first 50 μm below the pia.[34]

a. Select a region that is away from the dendritic tuft end or the branching region.

Note: This step will reduce spine density variability within individual dendritic shaft segments.

b. Use the cell fill channel in the eye-port of the microscope to find a dendritic shaft segment that measures at least 30 μm, parallel to the horizontal plane, as much as possible, so that much of the segments is located within a few Z steps.

Note: This will reduce the spine density variability within dendritic shaft segments, decrease imaging time and homogenize artifacts from optical aberrations within the ROI.

c. Choose dendritic segments that are isolated from other cells.

Note: "Busy" images with several dendrites around and across the dendrite of interest will make reconstruction much more difficult. The user can increase the sparseness of transfected cells in L2/3 by optimizing IUE plasmid concentration or the parameters of the voltage pulses applied during the IUE.[5]

Note: If the user is experimenting with Cre-dependent constructs to obtain sparse expression, they can optimize the ratio of the plasmids containing Cre recombinase and the Cre-dependent construct.[35]

4. Once a dendrite is chosen, set the Z stack according to the cell fill channel, adding a few sections of space above and below the dendrite to image its entirety without question.

Note: In our protocol, this is accomplished by acquiring images from dendritic shafts and synaptic markers localized to apical dendritic tufts in L1 as stacks of approximately 20–60 optical sections (Z-step = 0.2 µm) with an XY resolution of 10 px/ µm.

Note: When imaging both the dendrite and puncta, excitation and STED laser power for each channel should be set to levels in which the readout of the signal intensity after a single scan is bright but does not result in photobleaching.

⚠ CRITICAL: If the system utilizes a photon-counting detector mode, the excitation and STED laser power should be set so that it does not result in a nonlinear relationship between photon counts and excitation. In the case of the Abberior Imspector software, the excitation should be brought up so that the "counts" readout is not much more than 100 for a single scan (see Note below). We recommend determining which confocal excitation power setting for a channel result in approximately 100 or so counts (a confocal test).

⚠ CRITICAL: If one is using a system with a different readout of signal intensity, we recommend determining a confocal excitation power setting that results in a signal that is midway between too dim to see and oversaturated after a signal scan, so that signal averaging or set scan accumulations may be set without photobleaching the sample (please see "optimizing confocal imaging parameters guide" section for detailed instructions and imaging tips).

When using the Abberior STED Facility line system, the period during which photons are counted in response to each excitation pulse is approximately 27 ns. Avalanche photodiodes can only detect a single photon during that period as they need to be electronically reset to detect a second one. This necessitates measures to ensure that the probability of missing photons is very low. Therefore, we suggest that about half of the intervals are blank. Considering these 27 ns periods are repeated for 5 µs, we recommend keeping the photon counts to approximately 100 for the 5 µs period as a rule of thumb. Higher counts will not affect the location of the labeled proteins but will affect the relative brightness. Therefore, a linear range of counts should be implemented if quantification of fluorescence is desired. To do this

5. Double the above confocal excitation power value for the STED excitation.
6. Set the STED depletion laser power setting at a level that does not detract from the counts given by the confocal test, i.e., addition of the STED depletion laser should not result in lower signal intensity than the confocal test and does not degrade the image (based on the confocal test).

   Note: We recommend determining the STED depletion laser power via trial and error with practice areas that won't be used for analysis.

   Note: Accumulations/averaging of the signal should be set to provide the brightest image without bleaching the fluorophores. To do this, the user should test excitation/averaging combinations on practice areas that will not be used for analysis.

STED dendrite imaging

Timing: ~1 h/image

This step describes the strategy for super-resolution STED imaging and analysis of the dendrite for the determination of neuronal morphology (Figure 3) (**Question 1**).

7. To select and image a dendritic ROI, follow the steps in the previous "imaging" section.

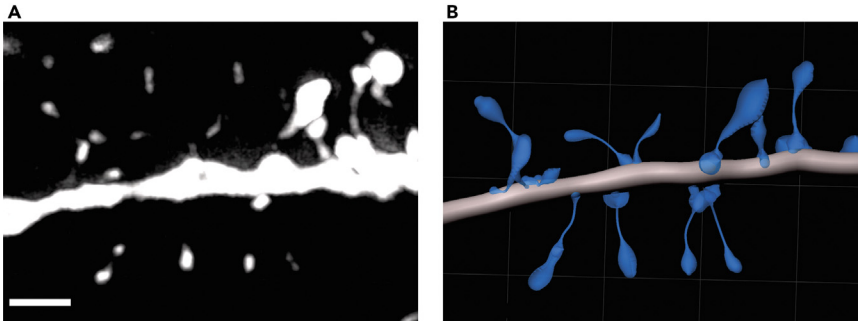

Figure 3. Dendrite imaged with STED then reconstructed in Imaris (Question 1)
(A) GFP-positive dendrite from a transfected L2/3 neuron in the mPFC stained with anti-GFP primary and Abberior STAR Orange secondary, then imaged with STED.
(B) Reconstructed dendritic spines in Imaris with semi-automatic filament reconstruction (described in the protocol). For both images, scale bar = 0.7 μm.

Note: Using the IHC protocol described above, we stain transfected EGFP-positive cells and processes with an anti-GFP primary (1:500) and corresponding Abberior STAR Orange or STAR Red secondary (1:300 STAR Orange, 1:1000 STAR Red). This approach allows the cell fill signal to be compatible with STED imaging.

Note: Considering the size and shape of dendritic structures to be imaged with STED, one must be cognizant of the power to counts ratio for resolving small structures such as necks without bleaching the sample. The user should remember that the spine necks will be dimmer relative to spine heads (Figures 3 A and 3B).[4,10,36]

Note: Optical aberrations can be further reduced by combining STED with hollow Bessel beams, or adaptive optics described elsewhere.[37–39]

EXPECTED OUTCOMES

Here, we provide a pipeline to perform morphological super-resolution imaging and Imaris analysis of dendritic spines and protein clusters in L1 apical tufts of L2/3 pyramidal cells. Once the user completes the pipeline, it will have access to several parameters that can be used to determine spine density and morphology, identify protein clusters and determine their size, determine the localization of the protein clusters in the dendrite, and the colocalization of two protein clusters[3,10,33,40–42] (Figure 4).

Using this approach, we determined that the spine density of a representative L1 apical dendrite in the mPFC is 2.18 spines/ μm (Question 1 and Figures 4 A–D). Additionally, our data shows that 31% of dendritic GluR1 was colocalized with LAMP1, and 23% of dendritic LAMP1 was colocalized with GluR1 (Figures 4 A–D), suggesting that a subpopulation of AMPA GluR1 subunits is being degraded in the lysosome of L1 spine apical tufts (Question 2). Our analysis pipeline also provides a distribution of protein cluster sizes for GluR1 and LAMP1 (Figures 4 E and F; Volume: GluR1: 0.018 ± 0.0070 μm^3; LAMP1 0.0059 ± 0.0060 μm^3, n = puncta).

We used other parameters to measure the colocalization of two protein clusters (Question 2), including the average minimum distance between dendritic GluR1 and LAMP1 clusters and the average overlap volume between dendritic GluR1 and LAMP1 surfaces (Figures 4 D, G, and H). For two protein clusters, decreased minimum distance and increased overlap volume suggest increased colocalization, which in our case, can be used to make conclusions about the degradation of synaptic proteins. For one representative dendrite, we found that the average minimum distance between GluR1 and LAMP1 was 0.5510 ± 0.04 μm, and the average overlap volume

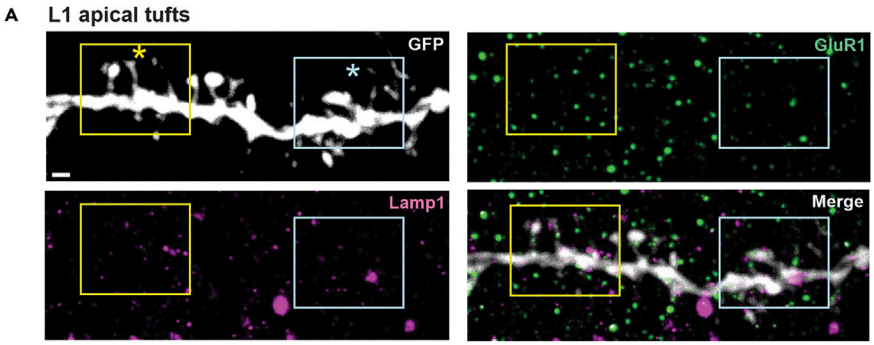

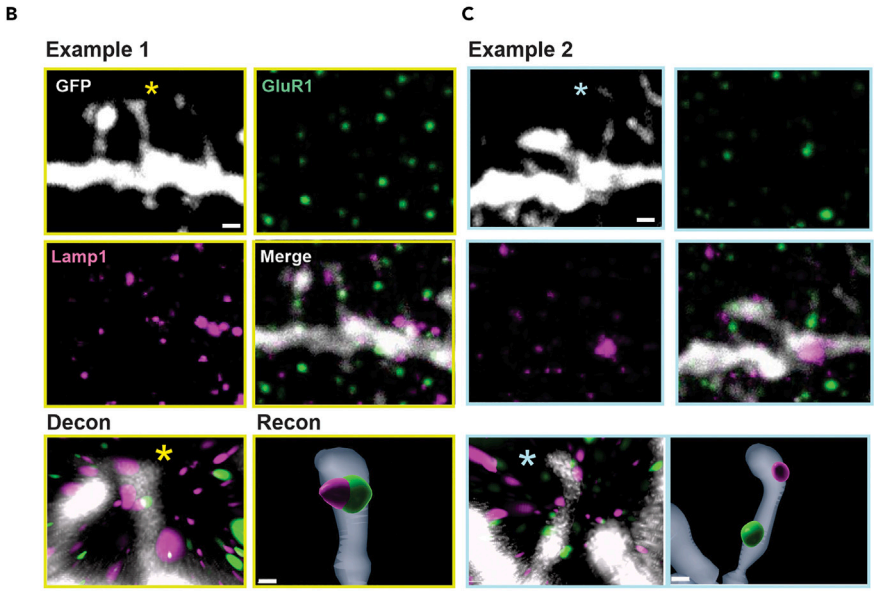

D

Overlap volume between GluR1 and LAMP1 (avg)	0.2560 μm^3
Minimum distance between GluR1 and LAMP1 (avg)	0.5510 μm^3
GluR1 in spine head versus neck	40%
LAMP1 in spine head versus neck	41%
GluR1 volume (avg)	0.0148 μm^3
LAMP1 volume (avg)	0.0059 μm^3
Dendritic GluR1 colocalized with LAMP1	31%
Dendritic LAMP1 colocalized with GluR1	23%
Spine Density	2.18 sp/μm

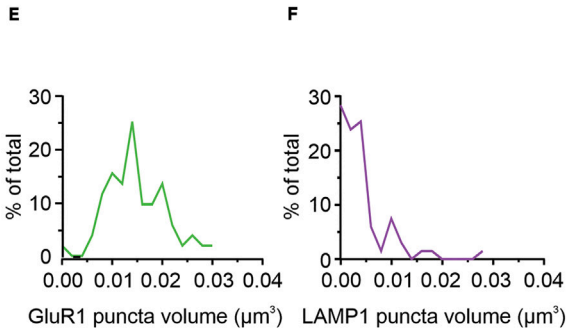

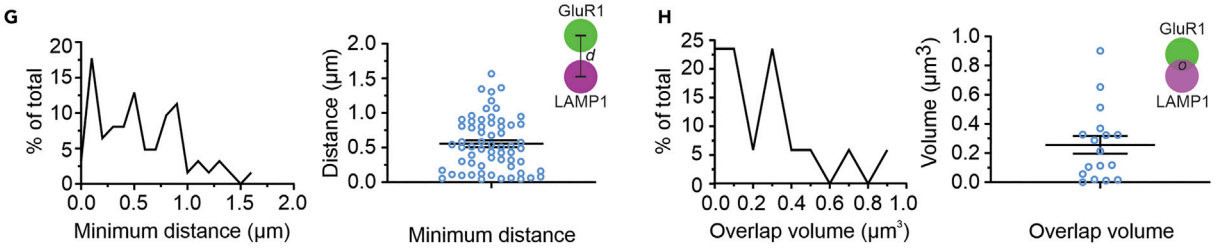

Figure 4. Colocalization of GluR1 and lysosomal clusters in L1 apical tufts

(A) Representative 60× STED image of an Apical Tuft stained with GFP (white, non-STED channel), GluR1 (green), LAMP1 (magenta) (Scale bar = 1.5 μm).
(B and C) Yellow and cyan squares show examples of dendritic spines with GluR1 and LAMP1 clusters that colocalize (Left, example 1, yellow asterisk) and that do not (Right, example 2, cyan asterisk). (B) Scale bar = 250 nm. (C) Scale bar = 100 nm.
(D) Selected parameters extracted from the analysis pipeline.
(E and F) Frequency distribution of GluR1 and LAMP1 puncta volumes.
(G) Frequency distribution and scatter plot of minimum distances between colocalized puncta. Schematic showing minimum distance (d) between two puncta.
(H) Frequency distribution and scatter plot of overlap volumes between colocalized puncta. Schematic showing overlap volume between two puncta (**Questions 2 and 3**). L. layer; Decon, deconvolution; Recon, reconstruction.

between dendritic GluR1 and LAMP1 surfaces was 0.2560 ± 0.0609 μm (Figures 4D, 4G and 4H, n = puncta).

For a representative dendrite, we also show the distribution of minimum distance and overlap volume (Figures 4G and 4H), which supports the conclusion that the lysosome is degrading a subpopulation of AMPA GluR1 subunits in L1 apical tufts (Question 2). Lastly, we determined the nanoscale organization of specific synaptic and endo-lysosomal proteins within dendritic subcompartments (Question 3). Our data shows that 40% of the dendritic GluR1 was in the spine head versus the neck, and 14% of the dendritic LAMP1 was in the spine head versus the neck (Figures 4A–4D).

We present a comprehensive pipeline for the imaging and analysis of brain slices, utilizing the powerful combination of super-resolution STED microscopy and Imaris software. Brain slices provide a superior experimental model for unraveling the complexities of neurological diseases. By employing STED microscopy in conjunction with Imaris, we demonstrate a highly accessible approach to cracking the nanoscale organization of synaptic proteins.

QUANTIFICATION AND STATISTICAL ANALYSIS

ImageJ file conversion

Timing: 5 min/image

The Abberior Imspector software saves images as .obf files, while the Leica SP8 STED software saves images as .lif files. Depending on the system used, images may need to be converted to .tif to be used in Imaris. In our case, we utilize the following approach to converting .obf files to .tif format.

1. Open FIJI/ImageJ and import the 3-channel image acquired from the STED microscope.
2. Use the color tool to merge the three channels, in our case: STAR Orange (GluR1), (Pseudo Colored green), Alexa 488 (EGFP IUE cell fill), (Pseudo Colored white), and STAR Red (LAMP1) (Pseudo Colored Magenta).
3. Once channels are merged, convert the image to 32-bit format.

Note: While Imaris can utilize images of other bit depths, we recommend converting the images to 32-bit as they are of floating-point format, meaning information stored in this way may avoid rounding errors associated with, for example, a 16-bit fixed-point format.

4. Save file as .tif to convert the file to the .tif format.

Imaris image processing and deconvolution

Timing: ~15 min/image

Imaris is an interactive microscopy image analysis software boasting several packages for various biological investigations from cancer research to cellular biology. Imaris for Neuroscientists is a package that enables 3D reconstruction of cells and cellular structures and analysis of various features, such as dendritic spine morphology and arborization complexity. In addition to included modules, this protocol requires free downloadable Imaris Extensions such as Colocalize Spots and Spots close to Filaments (Full list of necessary Imaris Extensions in key resources table).

Note: Convolution within the context of microscopy is a mathematical operation combining a PSF with the real object of interest and system noise.[3] Deconvolution, on the other hand, attempts to use algorithms to reverse this process by separating the PSF and the actual object from the convolved image, effectively reducing the influence of system noise. By undoing the blurring effects and isolating the desired signal, deconvolution helps improve the image's clarity and fidelity. Deconvolution is most often achieved by considering the factors that caused the convolution (pinhole size, objective magnification, immersion media, etc.) and using algorithms to "work backward", providing a reliable estimate of the image sharpness.[3]

While numerous deconvolution software and algorithms are available, this protocol was optimized for using Imaris iterative deconvolution algorithm. In principle, iterative algorithms estimate the original image, blur it using the system's PSF and compare the blurred estimate to the original image. With each iteration of this process, the estimated image is updated.

5. In the Observe Folder view, select the folder containing the .tif file of interest.
6. Double click the file to convert it to .ims (Imaris' native format).

Optional: The 3 channels can be pseudo-colored for ease of analysis. As an example, for Questions 2 and 3, we set the dendritic shaft as white, the synaptic marker as green, and the lysosomal marker as magenta.

Imaris dendritic shaft and spine reconstruction

Timing: ~1 h/image

This step describes the digital reconstruction of the dendrite fluorescence data in Imaris (Figure 5, Methods video S1) (**Question 1**). This allows the calculation of dendrite morphology parameters for analysis (described below).

7. Open the slice view of Imaris, then use the line tool to measure several wide parts of the neuronal dendrite, then the narrowest parts. Make note of these values for step 4.
8. Create a new filament object.
9. Select the source channel used to image the neuron, in our case channel 2.
10. Input largest diameter and thinnest diameter values from step 1.
11. Drag dendrite starting points threshold to the right until all are gone, then "shift + right click" to add a starting point on the preferred starting point for reconstruction.
12. Drag dendrite seed points threshold until seed points adequately populate the dendrite shaft, using "shift + left click" to remove unwanted points from other parts of the image (Figure 5 B).
13. Adjust diameter threshold until visualization adequately coats the dendrite (Figure 5 C).
14. Complete dendrite shaft reconstruction without seeding spines.
15. Select the Draw tab of the filament channel used for the dendrite reconstruction.
16. Select AutoPath for Method.
17. Select Spine for Type.
18. Select cell fill channel (or channel 2 in our case) for the source channel.
19. Under Correction, select Automatic Center and Automatic Diameter.
20. "Shift + right click" to add the base of the spine (Figure 6 A).

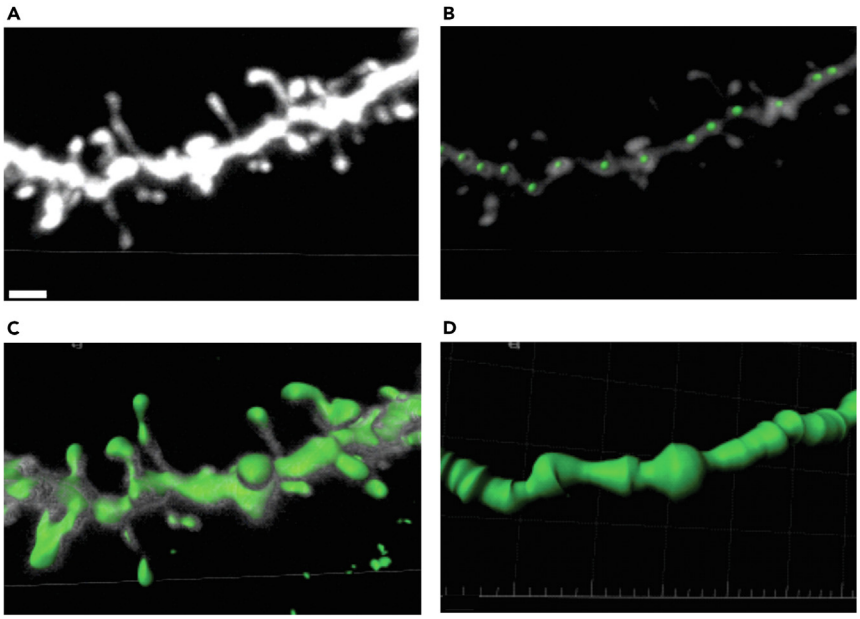

Figure 5. Dendrite shaft reconstruction (Question 1)
(A) Representative GFP-positive dendritic segment.
(B) Fluorescent signal for dendrite segment (intensity lowered for visualization purposes) and seed points for dendritic shaft (green spots).
(C) Visualization of dendritic shaft threshold adjusted according to fluorescence signal.
(D) Resulting dendritic shaft reconstruction. For all images, scale bar = 0.5 μm.

21. Shift "left click" to add the end of the spine (Figures 6A and 6B; The yellow line represents the automatic recognition of the spine fluorescence data).
    a. Once all the spines are manually inserted in this way, recalculate spine diameters in a similar manner as the dendrite diameter calculation shown in Figures 6C and 6D by clicking Spine Diameters under the Create tab.

Note: Through trial and error, we have found that manually inserting the spines rather than seeding them results in more accurate reconstructions for our data. However, either method may be used per the best judgment of the investigators.

Imaris puncta reconstruction

Timing: ~30 min/image

In our protocol, imaged puncta represent protein clusters. Their reconstruction in 3D space using Imaris allows us to obtain information regarding their sizes and location within dendritic spines (e.g., spine head versus neck). Puncta can be reconstructed using two methods in Imaris: spots (for the proper determination of puncta position) and surfaces (for the proper determination of puncta morphology). To ensure the most trustworthy analysis of surface and spot reconstructions, puncta are reconstructed as surfaces and spots, the spots are filtered according to the surfaces and the surfaces are then filtered according to the resulting spots (Figure 7, Methods video S1).

22. Create a new surface object.
23. Select source channel of interest (in our case Channel 1).
24. Under the thresholding tool, select Background Subtraction (Local Contrast), with 0.18 μm as the Diameter of largest Sphere which fits into the Object.

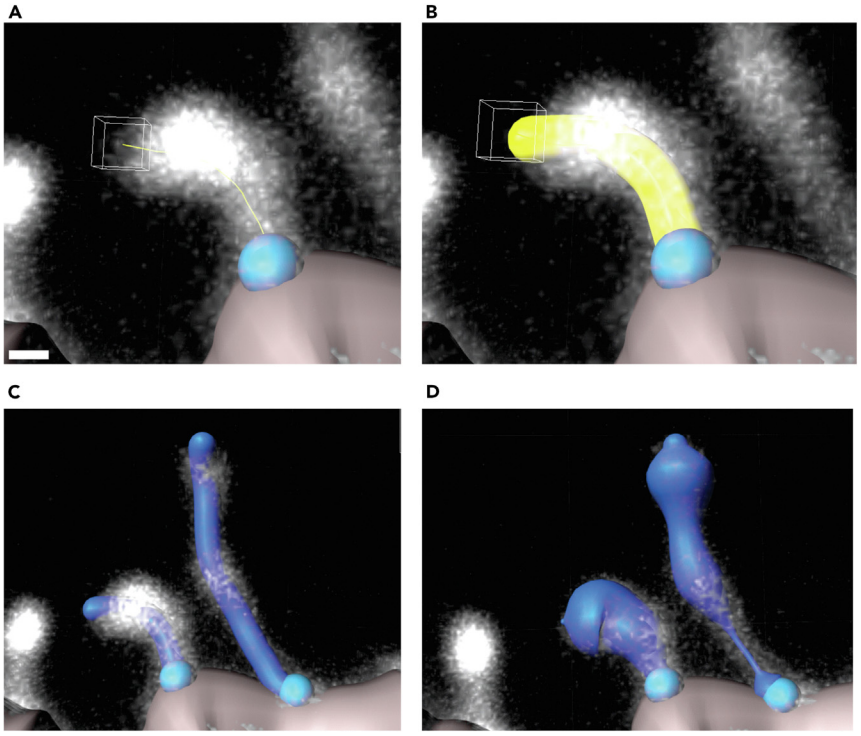

Figure 6. Dendritic spine reconstruction (Question 1)
(A) Spine start point (blue ball) for a dendritic segment.
(B) Spine reconstruction after "shift + right click" for manual insertion from A.
(C) Reconstruction of two dendritic spines before diameter recalculation.
(D) Reconstructions from panel C after diameter recalculation. For all images, scale bar = 0.5 μm.

25. Set threshold so that threshold visualization adequately coats the fluorescence data.
26. Set lower voxel limit to 60.

Note: The value of 0.10 μm for the Diameter of largest Sphere which fits in the Object (Imaris' default measure of size for surface reconstructions) and 60 for the lower voxel limit suits most surface puncta reconstructions for our purposes but may be adjusted for other applications.

27. Delete classification filter.
28. Create a new spots object.
29. Use default creation parameters.
30. Under Algorithm Settings, make sure Classify Spots and Object-Object Statistics are selected.
31. Select source channel of interest (in our case Channel 1).
32. Open slice view of Imaris, then use the line tool to measure several puncta at multiple planes. Note down the average XY diameter of puncta.
33. Under Spot Detection, enter the value from Step 11 in the box for Estimated XY Diameter, in our case 0.11 μm (the estimated diameter of GR1 puncta, obtained from our cluster size distribution analysis).
34. Set threshold so that spots adequately populate the punctate fluorescence signal.

⚠ CRITICAL: The threshold settings in steps 4 and 13 (steps above) can be determined in a variety of ways. We chose these values with a size distribution analysis of each puncta type by setting visual thresholds for 5 example images. We then fitted a Gaussian curve to the

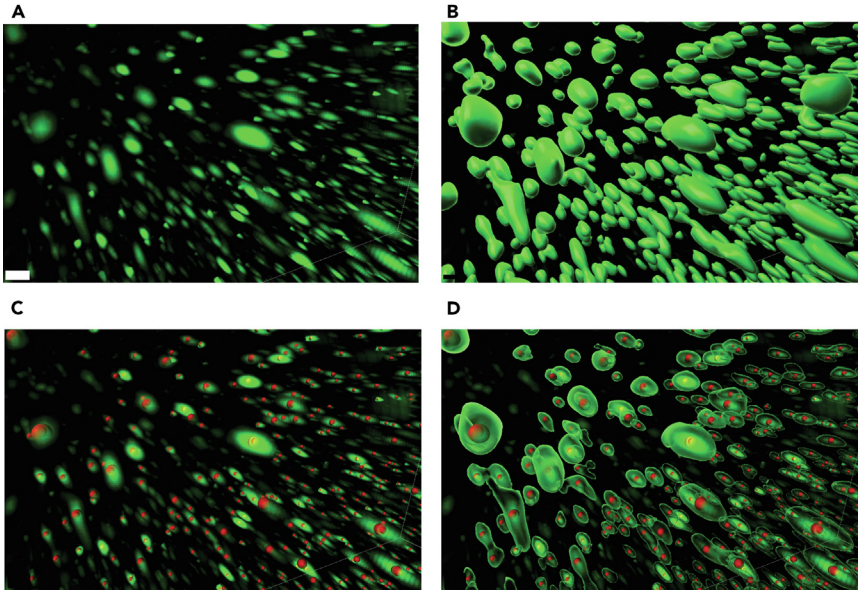

Figure 7. Surface and spot reconstruction (Questions 2 and 3)
(A) GluR1 signal alone (green).
(B) Filtered surface reconstruction of GluR1 signal.
(C) Filtered spot reconstruction of GluR1 signal (red) merged with GluR1 signal (green).
(D) Surface and spot reconstructions merged with GluR1 signal. For all images, scale bar = 0.3 μm.

obtained distribution to calculate the mean puncta sizes. This threshold can also be determined according to a visual assessment of the fluorescence data. We recommend investigators use trial and error with multiple methods to determine which suits their applications best.

35. Delete classification filter.
36. In the newly created spots object, add a filter.
37. For Filter Type, select Shortest Distance to Surfaces Surfaces = Surfaces 1".
38. Turn off the lower threshold limit, then adjust the upper limit so that only those spots inside surfaces are selected.
39. Click Duplicate Selection to new Spots.
40. Delete old spots object and rename this new duplicated spots object.
41. In the surface object, add a filter. For the Filter Type, select Shortest Distance to Spots = Spots 1".
42. Turn off the lower threshold limit, then adjust the upper limit so that only those surfaces encapsulating the thresholded spots are selected.
43. Click Duplicate Selection to new Surfaces.
44. Delete old surfaces object and rename this new duplicated surfaces object.

Imaris dendritic puncta filtering and colocalization

Timing: ~30 min/image

The following steps are required to continue the processing of puncta as spots. The user will need the find *Spots Near to Filament Border* and *Colocalize Spots* Imaris Extensions, available on the Imaris open website. This step filters spots and surfaces to only analyze the puncta that are associated with the dendrite (Figure 8, Methods video S1). This step allows for the determination of puncta localization within the dendritic spines and shaft in later steps (**Questions 2 and 3**).

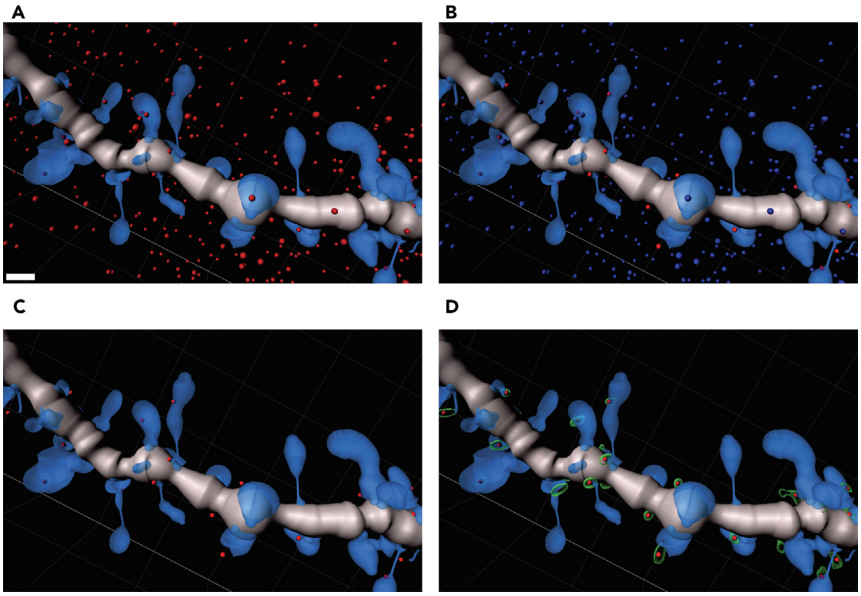

Figure 8. Dendritic spot and surface filtering (Questions 2 and 3)
(A) Dendrite reconstruction (blue/gray) with filtered GluR1 spots reconstruction (red).
(B) Results of Spots Close to Filament Border XTension: farther than threshold (blue) and closer than threshold (red).
(C) Spots closer than the "dendritic" threshold isolated. D) Dendritic spots with dendritic surfaces. Scale bar = 1 μm.

45. In the newly created spots object, go to Extensions and select Find Spots close to Filament Border Extension.
46. Input threshold distance of interest.
47. Delete spots object farther than the threshold cutoff.
48. Rename spots object closer than the threshold cutoff as Dendritic Spots.
49. Turn on Dendritic spots and turn off all other spots objects.
50. Make the surfaces object of interest translucent and the Dendritic Spots a contrasting color.
51. With the Edit tab selected, "control + click" the surfaces encapsulating the Dendritic Spots.
52. Once all the relevant surfaces are selected, click duplicate.
53. Rename the duplicated channels as Dendritic Surfaces.
54. Click on one of the spots objects of interest.
55. Go to Extensions and select the Colocalize Spots Extension.
56. Shift + "left click" the two spots objects (selecting them both at once) of which to determine co-localization.
57. Enter the distance threshold.

⚠ CRITICAL: The threshold distance settings in steps 2 and 13 are unique to the structures of interest. We determined these values using the size distribution analysis described in the previous section. These thresholds can also be determined according to measuring of the puncta in the slice view. We recommend investigators use trial and error with multiple methods to determine which suits their applications best.

Imaris puncta surface cutting

Timing: ~30 min/image, depending on puncta density

When puncta are reconstructed as surfaces in Imaris, they are sometimes inaccurately represented as multiple puncta in one surface. This can be remedied by using the surface cutting tool (Figure 9).

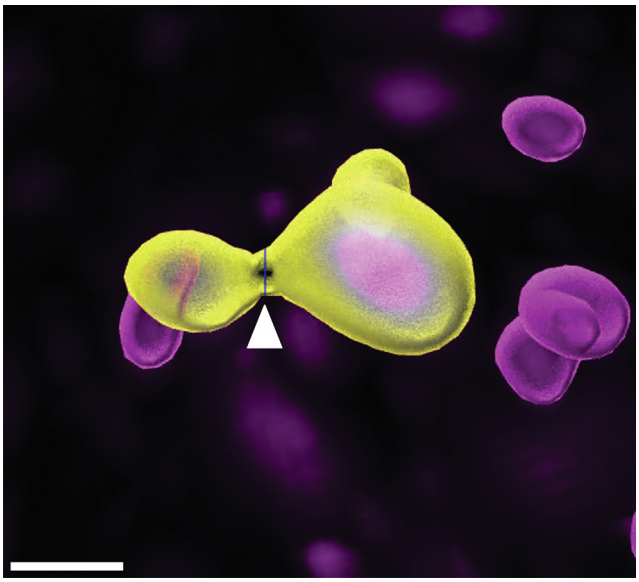

Figure 9. Puncta surface cutting (LAMP1, magenta) (Questions 2 and 3)
White arrow points to blue line indicating site of cut. Yellow, selected puncta. Scale bar = 0.2 μm.

We recommend performing this step after surfaces are filtered to limit cutting to only those surfaces that will be analyzed/exported (**Questions 2 and 3**).

58 Select the surface object containing the puncta of interest.
59 Select the "edit" tab.
60. The cutting tool is always a vertical line, so the puncta must be oriented so that the correct cut is positioned vertically.
61. Shift + "left click" to set the line to be cut.
62. In the "edit" tab space, select "cut".

Imaris data exporting

Timing: ~30 min to 3 h/image, depending on puncta density

This step allows for the analysis of fluorescence data for the analysis of dendrite morphology and the determination of puncta localization within the dendrite (spine head, spine neck, dendritic shaft). This also allows for the determination and manipulation of numerous data parameters including but not limited to puncta surface area, volume, overlap with neighboring puncta, etc. (**Questions 2 and 3**).

⚠ CRITICAL: To ensure proper compatibility with the custom MATLAB code (described below), files must be organized in the following manner per analyzed dendrite (Figure 10).

63. First make a folder for the staining condition (e.g., "GR1 + LAMP1").
64. Next make a folder for the experimental condition, in our case titled "All Imaris Statistics".
65. Within this folder, there must be a folder for each dendrite.
66. Within this folder, there must be four folders for each major data export.
    a. Filament (for dendrite and spine morphology data)
    b. Puncta stain 1 (in our case, "GR1")(for localization data, to be explained below)
    c. Puncta stain 2 (e.g., LAMP1)(for localization data, to be explained below)

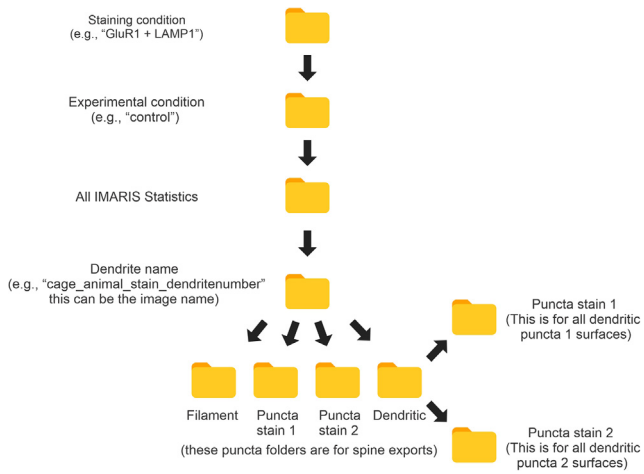

Figure 10. Schematic of file path organization for Imaris data exporting (Questions 1–3)
This organization scheme must be followed to ensure compatibility with the custom MATLAB code.

d. Dendritic, within this folder there must be two sub folders:
   i. Puncta stain 1 (for all dendritic surfaces of puncta 1)
   ii. Puncta stain 2 (for all surfaces of puncta 2)

67. In Imaris, click on the filament object.
68. Click on the Statistics tab.
    a. Make sure Overall is highlighted.
69. Click Export All Statistics to file.
70. Use the name of the image for the exported file and save in the filament folder described above.
71. Click on a spine of interest.
72. Click on the Statistics tab.
73. Click Selection.
    a. Make sure Specific Values is selected.
74. Select Spine Length.
75. Note down the last 5 digits of the spine ID number.
76. Click the surface of interest associated with the spine.
77. Click the Statistics tab.
    a. Make sure Overall is selected.
78. Click Export All Statistics to file.
79. Make sure the file name is formatted in the following way depending on if the puncta are in the head or neck of the spine:
    a. "last5digitsofID_head/neck" (e.g., 00051_head)

Note: We found the naming scheme described in Step 17 useful for our purposes as it allowed us to keep track of both the spine ID and location in the spine at the same time, but one could also develop their own naming scheme with information for other methods of organization.

80. Save the file in the folder corresponding to the puncta type as described above.
81. Do this for all puncta associated with spines. If there are multiple puncta in the head or neck, use "control + click" to select all the head or neck puncta and save them using the spine ID method described in step 17.
82. Repeat steps 9–19 for the next puncta type.
83. Click on the "Total Dendritic" surface object of interest.
84. Click the Statistics tab.
    a. Make sure Overall is selected.

18. Click Export All Statistics to file.
19. Use the name of the image for the exported file and save in the Puncta folder within the dendritic folder described above.
20. Repeat steps 21-24 for all punctum types.

MATLAB analysis of Imaris exported data

Timing: ~15 min/image

To maximize the information obtained from data exported using Imaris, we wrote a custom MATLAB script along with supporting functions (see key resources table). The script can be run on any version of MATLAB after the supporting functions are added to path. The script is run as follows.

8. In MATLAB, run the first section of the script using the "Run Section" button or by pressing "Control + Enter."
9. Select the folder with the correct staining condition (e.g., folder titled "GR1 + LAMP1") in the folder box that pops-up.

Note: Line number 20 of the code (explained further in the GitHub README file, https://github.com/CruzMartinLab/IMARIS_compiler) will decide which condition in the staining folder will be excluded from analysis.

9. After the first section completes running, run the second section. This section will result in several files in the workspace, of which the following are the required output:
   a. Average_parameters:

Note: Provides information about dendrite length, spine density, spine length, spine volume, average minimum distance between the two stained puncta, average overlap volume between the puncta, average colocalized volume ratio for colocalized puncta.

   b. All_synaptic_parameters:

Note: Provides information about the number of synaptic puncta occurring in the spine head or neck for each dendrite, their average volumes, and their average areas.

Note: In our case "GR1" is referred to as synaptic. In general, in the folder naming scheme, the first stain named is termed synaptic.

   c. All_compartment_parameters:

Note: Provides information about the number of synaptic puncta occurring in the spine head or neck for each dendrite, their average volumes, and their average areas.

Note: In our case LAMP1 is referred to as compartment. In general, in the folder naming scheme, the second stain named is termed compartment.

   d. Spine_classification_synaptic:

Note: Classifies spines based on number of compartment termed puncta (as described above) in each spine.

Note: histo_len*: There are 14 of these in total. They provide information on individual spine parameters for every dendrite for all metrics mentioned above in Average_parameters.

⚠ CRITICAL: To run the code for a different condition or for a different stain, rerun the first section with required changes as suggested in the GitHub README file, https://github.com/CruzMartinLab/IMARIS_compiler.

LIMITATIONS

Cellular dynamics

One limitation of our methodology is that fixing the tissue does not allow us to capture the activity-dependent dynamics of spines and protein clusters and GluR1 recycling in the postsynaptic compartments.[1,4]

Tissue fixation

Formaldehyde brain fixation can alter the 3D structure of cells and tissues and affect the availability of antigens for immunostaining and antibody penetration.[48] Although the effects of PFA on the brain's structure are often overlooked, the experimenter must consider these aspects when designing IHC experiments. Fortunately, a few studies have made breakthroughs, allowing users to overcome often-encountered obstacles. For example, Lai et al.[9] have developed a scalable method to stabilize antibodies (SPEARs) against thermal and chemical denaturation, allowing them to withstand prolonged exposure to high temperatures and harsh denaturants. This advancement enables dynamic modulation of antibody properties, facilitating faster deep tissue immunolabeling and broader compatibility with various tissue processing methods.[9]

Additionally, glyoxal fixation greatly enhanced antibody penetration and immunoreactivity compared to the gold-standard formaldehyde fixative, particularly enabling the detection of buried molecules in brain tissue.[50] An additional advantage of glyoxal is that it acts faster than formaldehyde, cross-linked proteins more effectively, and improves the preservation of cellular morphology.[8]

Antibody selection

Considering the previously mentioned stringent tissue preparation guidelines for proper STED microscopy (tissue thickness, coverslip mounting, etc.), antibody selection for STED must be more particular than that for traditional IHC experiments. For example, STED optics is optimal in thin-sliced tissue, so primary antibodies should be selected and tested with proper penetration and SNR kept in mind. As mentioned previously, secondary antibodies should be selected based on their compatibility with STED depletion technology, which could limit possible antibody combinations for certain experiments. It should be mentioned that fluorophore choice for structures of interest should also be kept in mind due to differences in strength between the red and far red lasers that may exist within a particular STED set up, such as the relatively weaker far red laser (in our case, acting on the Abberior STAR Orange) of our Abberior Facility line system necessitating higher power and signal accumulation settings for that channel as compared to the red laser (in our case, acting on the Abberior STAR Red). Antibody testing and optimization should be performed thoroughly prior to the acquisition and analysis of experimental data.

STED imaging

One of the most salient limitations is that of STED channel availability. The Abberior Facility line system that we used can only maintain two STED channels at a time due to only two available STED lasers. F5 has been difficult to use as a STED fluorophore (but see Rankin et al.[32]). Although we do not use F5 to perform super-resolution imaging of dendritic spines, we use this fluorophore to determine the location of protein clusters in the dendrite. STED imaging tends to dim small-volume structures such as spine necks. To improve spine neck signal, we suggest optimizing antibody staining parameters and improving SNR (see "optimizing confocal imaging parameters guide" and "imaging and STED dendrite imaging" section).

Imaris analysis

Limitations regarding Imaris are those of accessibility to the software and proper computer processing power. Imaris is expensive, and while it is most certainly a good investment for labs and departments alike, we recognize that labs may not have the funds either individually or in a community to access the software. Furthermore, users might not have access to high performance computer processing power, which can have a significant impact of analysis time. If a lab has access to Imaris, we strongly recommend utilizing a computer with specifications matching or exceeding those recommended by Oxford Instruments for ease of analysis and reduced errors.

There are several alternatives to Imaris for the morphological analysis of cellular data, especially if budget constraints are a concern. Here are a few options: Fiji/ImageJ, CellProfiler (www.cellprofiler.org), KNIME (https://www.knime.com/community/image-processing), Microscopy, Image Browser (MIB, http://mib.helsinki.fi), and Python (https://www.pythonforbiologists.org), including scikit-image, OpenCV, and Cellpose.

TROUBLESHOOTING

Problem 1

Optical aberrations in STED images such as changes in spatial resolution and signal intensity (relevant to "optimizing confocal imaging parameters guide" and "imaging and STED dendrite imaging" section).

Potential solution(s)

Attempts to correct optical aberrations can be further achieved by combining STED with tissue-clearing approaches, hollow Bessel beams, or adaptive optics.[24,37–39] It is also important that the user images the most superficial horizontally aligned dendrites in the tissue.

Problem 2

Endogenous autofluorescent signals and non-specific autofluorescence (relevant to "optimizing confocal imaging parameters guide", "perfusion" section, and "imaging and STED dendrite imaging: section).

Potential solution(s)

Blood remnants in fixed brain tissue result in increased autofluorescent signals and reduced SNR. Therefore, it is crucial to remove blood from the fixed brain tissue properly. The user should ensure that the needles used to pump saline and PFA solution are not clogged and adequately positioned in the heart. Additionally, it is crucial to find an optimal perfusion rate that is not too weak or strong, paying attention to organ and tissue appearance and texture as the perfusion progresses.

To increase SNR during STED imaging, it is essential to decrease non-specific background fluorescence. Several actions that can be taken to reduce autofluorescence, namely: performing negative staining controls (see "antibody validation" section), prioritizing fluorophores that emit at wavelengths farther from the emission of autofluorescent endogenous molecules and pigments of the tissue (such as far-red selections),[30] and using background reducers such as TrueBlack, Sudan black B, or Eriochrome black T.[31]

Problem 3

The brain slices appear frayed with damage around the edges (sectioning of tissue – step 14).

Potential solution(s)

This is likely due to premature thawing of the brain during slicing. Make sure to keep the stage cold by continually adding ice to the stage and around the brain during slicing.

Problem 4

When constructing and filtering objects in Imaris, the object of interest is not listed as an option for filtering (Imaris puncta reconstruction).

Potential solution(s)

This is likely because filaments, surfaces, and spots were reconstructed and filtered out of order from what is listed in this protocol. Imaris is only able to filter a certain number of objects at a time, so it is essential that the filaments, surfaces, and spots are reconstructed and filtered in the order presented to ensure the proper objects are displayed when necessary.

Problem 5

MATLAB is reporting errors related to inabilities to find necessary files or file locations (MATLAB analysis of Imaris exported data – steps 1-3).

Potential solution(s)

While this could be due to several reasons, errors of these kind are most probably due to deviation from the critical file organization scheme described in the Imaris data exporting section and Figure 9. It should also be noted that naming strategies across all file handling steps must be kept consistent to avoid errors.

RESOURCE AVAILABILITY

Lead contact

Further information and requests for resources and reagents should be directed to and will be fulfilled by the lead contact, Alberto Cruz-Martı ´n (martini.cruz@gmail.com).

Materials availability

This study did not generate new reagents.

Data and code availability

The datasets supporting this study are available from the corresponding author upon request.

SUPPLEMENTAL INFORMATION

Supplemental information can be found online at https://doi.org/10.1016/j.xpro.2023.102707.

ACKNOWLEDGMENTS

We thank all research assistants in the Cruz-Martín lab. We thank Mike Kirber and the BU MED Cellular Imaging Core for using the STED microscope. We thank members of the Cruz-Martín lab for critical reading of the manuscript and helpful discussions. This work was supported by a National Institutes of Health R01 grant (NIH, R01MH127732) to A.C.-M. and a Brenton R. Lutz Award to R.A.P.

AUTHOR CONTRIBUTIONS

E.K. – conceptualization: formulated composition, goals, and scope of the paper and approaches for analyses; writing (original draft): wrote some parts of the original and revised draft; writing (review and editing): editing and feedback for the original and revised draft; visualization: figure design and generation; experiments: performed imaging experiments; and analysis: performed imaging analysis. R.A.P. – writing (review and editing): editing and feedback for the original and revised draft; visualization: figure design and generation; analysis: performed imaging analysis; and wrote and edited the original and revised computer code. A.B. – experiments: performed *in utero* electroporations to transfect L2/3 pyramidal cells with EGFP and writing (review and editing): editing and feedback for the original and revised draft. D.S. – analysis: performed imaging analysis (assisted with developing the Imaris reconstruction pipeline). O.I. – analysis: performed imaging analysis (assisted with STED image acquisition). A.C.-M. – conceptualization: formulated composition, goals, and

scope of the paper and approaches for analyses;writing (original draft): wrote some parts of the original and revised draft;writing (review and editing): editing and feedback for the original and revised draft;visualization: figure design and generation;supervision: mentorship and oversight of the project;project administration: management and coordination;and funding acquisition.

DECLARATION OF INTERESTS

The authors declare no competing interests.

REFERENCES

1. Nägerl, U.V., and Bonhoeffer, T. (2010). Imaging Living Synapses at the Nanoscale by STED Microscopy. J. Neurosci. *30*, 9341–9346.
2. Yang, X., and Annaert, W. (2021). The Nanoscopic Organization of Synapse Structures: A Common Basis for Cell Communication. Membranes *11*, 248.
3. Hruska, M., Henderson, N., Le Marchand, S.J., Jafri, H., and Dalva, M.B. (2018). Synaptic nanomodules underlie the organization and plasticity of spine synapses. Nat. Neurosci. *21*, 671–682.
4. Comer, A.L., Jinadasa, T., Sriram, B., Phadke, R.A., Kretsge, L.N., Nguyen, T.P.H., Antognetti, G., Gilbert, J.P., Lee, J., Newmark, E.R., et al. (2020). Increased expression of schizophrenia-associated gene C4 leads to hypoconnectivity of prefrontal cortex and reduced social interaction. PLoS Biol. *18*, e3000604.
5. Comer, A.L., Sriram, B., Yen, W.W., and Cruz-Martín, A. (2020). A Pipeline using Bilateral In Utero Electroporation to Interrogate Genetic Influences on Rodent Behavior. JoVE *159*, e61350.
6. Jeong, S., Widengren, J., and Lee, J.-C. (2021). Fluorescent Probes for STED Optical Nanoscopy. Nanomaterials *12*, 21.
7. Tønnesen, J., Nadrigny, F., Willig, K.I., Wedlich-Söldner, R., and Nägerl, U.V. (2011). Two-Color STED Microscopy of Living Synapses Using A Single Laser-Beam Pair. Biophys. J. *101*, 2545–2552.
8. Takasaki, K.T., Ding, J.B., and Sabatini, B.L. (2013). Live-Cell Superresolution Imaging by Pulsed STED Two-Photon Excitation Microscopy. Biophys. J. *104*, 770–777.
9. Vicidomini, G., Moneron, G., Han, K.Y., Westphal, V., Ta, H., Reuss, M., Engelhardt, J., Eggeling, C., and Hell, S.W. (2011). Sharper low-power STED nanoscopy by time gating. Nat. Methods *8*, 571–573.
10. Cruz-Martin, A., and Portera-Cailliau, C. (2014). In vivo imaging of axonal and dendritic structures in neonatal mouse cortex. Cold Spring Harb. Protoc. *2014*, 57–64.
11. Portera-Cailliau, C., Pan, D.T., and Yuste, R. (2003). Activity-Regulated Dynamic Behavior of Early Dendritic Protrusions: Evidence for Different Types of Dendritic Filopodia. J. Neurosci. *23*, 7129–7142.
12. Yap, C.C., Digilio, L., McMahon, L.P., Garcia, A.D.R., and Winckler, B. (2018). Degradation of dendritic cargos requires Rab7-dependent transport to somatic lysosomes. J. Cell Biol. *217*, 3141–3159.
13. Yap, C.C., Mason, A.J., and Winckler, B. (2022). Dynamics and distribution of endosomes and lysosomes in dendrites. Curr. Opin. Neurobiol. *74*, 102537.
14. Kopec, C.D., Real, E., Kessels, H.W., and Malinow, R. (2007). GluR1 links structural and functional plasticity at excitatory synapses. J. Neurosci. *27*, 13706–13718.
15. Lee, H.-K., Takamiya, K., He, K., Song, L., and Huganir, R.L. (2010). Specific Roles of AMPA Receptor Subunit GluR1 (GluA1) Phosphorylation Sites in Regulating Synaptic Plasticity in the CA1 Region of Hippocampus. J. Neurophysiol. *103*, 479–489.
16. Mead, A.N., Zamanillo, D., Becker, N., and Stephens, D.N. (2007). AMPA-Receptor GluR1 Subunits are Involved in the Control Over Behavior by Cocaine-Paired Cues. Neuropsychopharmacology *32*, 343–353.
17. Prakash, K., Diederich, B., Heintzmann, R., and Schermelleh, L. (2022). Super-resolution microscopy: A brief history and new avenues. Philos. Trans. A Math. Phys. Eng. Sci. *380*, 20210110.
18. Galbraith, C.G., and Galbraith, J.A. (2011). Super-resolution microscopy at a glance. J. Cell Sci. *124*, 1607–1611.
19. Calovi, S., Soria, F.N., and Tønnesen, J. (2021). Super-resolution STED microscopy in live brain tissue. Neurobiol. Dis. *156*, 105420.
20. Hell, S.W., and Wichmann, J. (1994). Breaking the diffraction resolution limit by stimulated emission: Stimulated-emission-depletion fluorescence microscopy. Opt. Lett. *19*, 780–782.
21. Wildanger, D., Bückers, J., Westphal, V., Hell, S.W., and Kastrup, L. (2009). A STED microscope aligned by design. Opt Express *17*, 16100–16110.
22. Bianchini, P., Peres, C., Oneto, M., Galiani, S., Vicidomini, G., and Diaspro, A. (2015). STED nanoscopy: A glimpse into the future. Cell Tissue Res. *360*, 143–150.
23. Wu, J., Cai, Y., Wu, X., Ying, Y., Tai, Y., and He, M. (2021). Transcardiac Perfusion of the Mouse for Brain Tissue Dissection and Fixation. Bio. Protoc. *11*, e3988.
24. Angibaud, J., Mascalchi, P., Poujol, C., and Nägerl, U.V. (2020). A simple tissue clearing method for increasing the depth penetration of STED microscopy of fixed brain slices. J. Phys. D Appl. Phys. *53*, 184001.
25. Bückers, J., Wildanger, D., Vicidomini, G., Kastrup, L., and Hell, S.W. (2011). Simultaneous multi-lifetime multi-color STED imaging for colocalization analyses. Opt Express *19* (4), 3130–3143.
26. Liu, T., Stephan, T., Chen, P., Keller-Findeisen, J., Chen, J., Riedel, D., Yang, Z., Jakobs, S., and Chen, Z. (2022). Multi-color live-cell STED nanoscopy of mitochondria with a gentle inner membrane stain. Proc. Natl. Acad. Sci. USA *119*, e2215799119.
27. Sednev, M.V., Belov, V.N., and Hell, S.W. (2015). Fluorescent dyes with large Stokes shifts for super-resolution optical microscopy of biological objects: A review. Methods Appl. Fluoresc. *3*, 042004.
28. Hoffman, G.E., Murphy, K.J., and Sita, L.V. (2016). The Importance of Titrating Antibodies for Immunocytochemical Methods. Curr. Protoc. Neurosci. *76*, 2.12.1–2.12.37.
29. Ghithan, J.H., Noel, J.M., Roussel, T.J., McCall, M.A., Alphenaar, B.W., and Mendes, S.B. (2021). Photobleaching reduction in modulated super-resolution microscopy. Microscopy *70*, 278–288.
30. Spitzer, N., Sammons, G.S., and Price, E.M. (2011). Autofluorescent cells in rat brain can be convincing impostors in green fluorescent reporter studies. J. Neurosci. Methods *197*, 48–55.
31. Davis, A.S., Richter, A., Becker, S., Moyer, J.E., Sandouk, A., Skinner, J., and Taubenberger, J.K. (2014). Characterizing and Diminishing Autofluorescence in Formalin-fixed Paraffin-embedded Human Respiratory Tissue. J. Histochem. Cytochem. *62*, 405–423.
32. Rankin, B.R., Moneron, G., Wurm, C.A., Nelson, J.C., Walter, A., Schwarzer, D., Schroeder, J., Colón-Ramos, D.A., and Hell, S.W. (2011). Nanoscopy in a Living Multicellular Organism Expressing GFP. Biophys. J. *100*, L63–L65.
33. Cruz-Martín, A., Crespo, M., and Portera-Cailliau, C. (2012). Glutamate induces the elongation of early dendritic protrusions via mGluRs in wild type mice, but not in fragile X mice. PLoS One *7*, e32446.
34. Cruz-Martín, A., Crespo, M., and Portera-Cailliau, C. (2010). Delayed stabilization of dendritic spines in fragile X mice. J. Neurosci. *30*, 7793–7803.
35. Chen, J.L., Villa, K.L., Cha, J.W., So, P.T.C., Kubota, Y., and Nedivi, E. (2012). Clustered dynamics of inhibitory synapses and dendritic spines in the adult neocortex. Neuron *74*, 361–373.
36. Phadke, R.A., Kruzich, E., Fournier, L.A., Brack, A., Sha, M., Picard, I., Johnson, C.,

Stroumbakis, D., Salgado, M., Liu, Y.Y., and Cruz-Martín, A. (2023). C4 Induces Pathological Synaptic Loss by Impairing AMPAR Trafficking. Preprint at bioRxiv. https://doi.org/10.1101/2023.09.09.556388.

37. Bancelin, S., Mercier, L., Murana, E., and Nägerl, U.V. (2021). Aberration correction in stimulated emission depletion microscopy to increase imaging depth in living brain tissue. Neurophotonics *8*, 035001.

38. Gould, T.J., Burke, D., Bewersdorf, J., and Booth, M.J. (2012). Adaptive optics enables 3D STED microscopy in aberrating specimens. Opt Express *20*, 20998–21009.

39. Yu, J., Sun, X., Cai, F., Zhu, Z., Qin, A., Qian, J., Tang, B., and He, S. (2015). Low photobleaching and high emission depletion efficiency: The potential of AIE luminogen as fluorescent probe for STED microscopy. Opt. Lett. *40*, 2313–2316.

40. Hruska, M., Cain, R.E., and Dalva, M.B. (2022). Nanoscale rules governing the organization of glutamate receptors in spine synapses are subunit specific. Nat. Commun. *13*, 920.

41. Li, B.-Z., Sumera, A., Booker, S.A., and McCullagh, E.A. (2023). Current Best Practices for Analysis of Dendritic Spine Morphology and Number in Neurodevelopmental Disorder Research. ACS Chem. Neurosci. *14*, 1561–1572.

42. Mao, Y.-T., Zhu, J.X., Hanamura, K., Iurilli, G., Datta, S.R., and Dalva, M.B. (2018). Filopodia Conduct Target Selection in Cortical Neurons using Differences in Signal Kinetics of a Single Kinase. Neuron *98*, 767–782.e8.

43. Biggs, D.S. (2010). A Practical Guide to Deconvolution of Fluorescence Microscope Imagery. Micros. Today *18*, 10–14.

44. Wegner, W., Ilgen, P., Gregor, C., van Dort, J., Mott, A.C., Steffens, H., and Willig, K.I. (2017). In vivo mouse and live cell STED microscopy of neuronal actin plasticity using far-red emitting fluorescent proteins. Sci. Rep. *7*, 11781.

45. Richter, K.N., Revelo, N.H., Seitz, K.J., Helm, M.S., Sarkar, D., Saleeb, R.S., D'Este, E., Eberle, J., Wagner, E., Vogl, C., et al. (2018). Glyoxal as an alternative fixative to formaldehyde in immunostaining and super-resolution microscopy. EMBO J. *37*, 139–159.

46. Melan, M.A. (1994). Overview of cell fixation and permeabilization. Methods Mol. Biol. *34*, 55–66.

47. Schnell, U., Dijk, F., Sjollema, K.A., and Giepmans, B.N.G. (2012). Immunolabeling artifacts and the need for live-cell imaging. Nat. Methods *9*, 152–158.

48. Tanaka, K.A.K., Suzuki, K.G.N., Shirai, Y.M., Shibutani, S.T., Miyahara, M.S.H., Tsuboi, H., Yahara, M., Yoshimura, A., Mayor, S., Fujiwara, T.K., and Kusumi, A. (2010). Membrane molecules mobile even after chemical fixation. Nat. Methods *7*, 865–866.

49. Lai, H.M., Tang, Y., Lau, Z.Y.H., Campbell, R.A.A., Yau, J.C.N., Chan, C.C.Y., Chan, D.C.W., Wong, T.Y., Wong, H.K.T., Yan, L.Y.C., et al. (2022). Antibody stabilization for thermally accelerated deep immunostaining. Nat. Methods *19*, 1137–1146.

50. Konno, K., Yamasaki, M., Miyazaki, T., and Watanabe, M. (2023). Glyoxal fixation: An approach to solve immunohistochemical problem in neuroscience research. Sci. Adv. *9*, eadf7084.